

## Regularities of solid-phase interaction of tin and molybdenum oxides: Catalytic properties

Kien Cuong Dao<sup>a</sup>, Alexander Aleksandrovich Il'in<sup>a</sup>, Ruslan Nikolaevich Rumyantsev<sup>a,\*</sup>, Ulyana Sergeevna Uzhevskaya<sup>a</sup>, Alexander Papvlovich Il'in<sup>a</sup>, Taisiya Andreevna Rumyantseva<sup>b</sup>

<sup>a</sup>Department of Inorganic Technology, Ivanovo State University of Chemistry and Technology, Sheremetievskiy Ave., 7, Ivanovo, 153000, Russia.

<sup>b</sup>Department of Technology of Fine Organic Synthesis, Ivanovo State University of Chemistry and Technology, Sheremetievskiy Ave., 7, Ivanovo, 153000, Russia.

Received 25 November 2018; received in revised form 9 January 2019; accepted 28 January 2019

### ABSTRACT

The interaction in the system of SnO<sub>2</sub> and h-MoO<sub>3</sub> prepared by their joint mechanical activation in a roller-ring vibratory mill was investigated. A series of catalysts was prepared with SnO<sub>2</sub>: h-MoO<sub>3</sub> molar ratio 1:1; 1:2.3; 2.3:1 and 5.7:1. The catalysts were characterized by various techniques including X-ray phase, X-ray diffraction (XRD) and synchronous thermal analysis, scanning electron microscopy (SEM), BET method. An important effect of the introduction of molybdenum atoms into the structure of SnO<sub>2</sub> was lattice defect. Heat treatment of the mechanically activated mixture at a temperature of 600–750 °C resulted in obtaining crystalline Sn(MoO<sub>4</sub>)<sub>2</sub>. The catalytic activity of the samples was investigated by the oxidative dehydrogenation of methanol. The results reported that varying the SnO<sub>2</sub>:MoO<sub>3</sub> ratio allows adjusting the selectivity of the methanol conversion process over methyl formate and dimethyl ether.

**Keywords:** Solid solution, SnO<sub>2</sub>, h-MoO<sub>3</sub>, Sn(MoO<sub>4</sub>)<sub>2</sub>, Mechanical activation, Catalytic properties.

### 1. Introduction

Tin and molybdenum oxides are widely used as catalysts for various chemical reactions, including partial oxidation of benzene, propene oxidation to acetone, as well as dehydrogenation and oxidation of methanol to formaldehyde and methyl formate [1-7].

For many catalytic reactions occurring on the solid surface of metals and their oxides, the greatest catalytic activity is observed when solid solutions of several oxides are used instead of individual oxides. Thus, during the oxidation of methanol to formaldehyde, the active phase is a solid solution of iron molybdate with an excess content of molybdenum oxide [8, 9]. The solid solution of SnO<sub>2</sub>-MoO<sub>3</sub> [10] possesses high catalytic activity in the methanol dehydrogenation reaction.

The influence of the conditions required for the tin-molybdenum catalysts preparation on their phase composition and catalytic activity [11] was investigated.

It was found that the mutual dissolution of tin and molybdenum oxides leads to a significant increase in their activity and selectivity in the selective oxidation reaction of propylene to acetone. It was shown [3] that the catalytic activity of the system weakly depends on crystalline tin oxide structures containing high concentrations of molybdenum. These catalytically active phases undergo the partial decomposition during the catalytic reaction with segregation of molybdenum (VI) oxide and loss of oxygen, which lead to the formation of anionic vacancies.

The production processes and properties of tin-molybdenum systems were studied [3, 7, 12, 13]. The tin molybdate catalyst with the molar ratio of SnO<sub>2</sub>:MoO<sub>3</sub> (Sn:Mo=9:1) [3] was prepared by the hydrothermal treatment of tin and molybdenum oxides suspension in water at 450 °C for 4 hours, and also by calcining the dry mixture. It was reported that the interaction between the oxides proceeds at a temperature of at least 450 °C.

The nature of the Bronsted and Lewis acid centers of the tin-molybdenum oxide catalyst was also discussed [12].

\*Corresponding author.

E-mail address: rnr86@yandex.ru (R.N. Rumyantsev)

Protons were suggested as Bronsted acid sites because they are acting as cations that compensate the charge of surface anions.

It is known that the mechanical activation (MA) not only increases the reactivity of a solid, but also initiates the solid-phase processes or significantly reduces the temperature of the subsequent heat treatment. In addition, the mechanical activation allows increasing the catalytic activity and selectivity of the formed contacts [1, 5, 14]. Despite numerous works in the field of preparation of tin-molybdenum catalysts for various compositions and studies of their catalytic properties in oxidation and dehydrogenation reactions, there are no data about the formation of tin-molybdenum solid solutions under solid-phase synthesis conditions using the mechanical treatment.

In this paper, we described the interaction between tin and molybdenum oxides at the stage of mechanical activation and subsequent heat treatment.

## 2. Experimental

### 2.1. Materials, equipment and sample preparation

The reagents and solvents used such as molybdenum oxide h-MoO<sub>3</sub> - 99.5 wt.% (Fe<sub>2</sub>O<sub>3</sub> and PbO as impurities) and tin oxide SnO<sub>2</sub> - 99.5 wt.% (Fe<sub>2</sub>O<sub>3</sub>, K<sub>2</sub>O and PbO as impurities) were supplied from Aldrich. A roller-ring vibration mill VM-4 (Czech Republic) was used for the samples preparation. The diameter of the grinding chamber was 98 mm, the total chamber volume was 0.302 dm<sup>3</sup>. The oscillation frequency was 930 min<sup>-1</sup>, the amplitude – 10 mm. The mass of grinding bodies was 1158 g, the mass of feed material was 50 g.

#### 2.1.1. Preparation of SnO<sub>2</sub>:h-MoO<sub>3</sub> catalysts

Samples with the molar ratios of SnO<sub>2</sub>:h-MoO<sub>3</sub> 1:1; 1:2.3; 2,3:1; 5.7:1. were prepared by the mechanochemical activation of a mixture of tin and molybdenum oxides in a roller-ring vibration mill VM-4 (Czech Republic) with further heat treatment at 750 °C within 60 min.

### 2.2. Characterizations

The SnO<sub>2</sub>:h-MoO<sub>3</sub> catalysts were characterized by different techniques. The XRD patterns of the catalysts were recorded on the DRON-3M (Russia) X-ray diffractometer. The CuK<sub>α</sub> radiation (λ=0.15406 nm, Ni filter), operating voltage and operating current of 40 kV and 20 mA respectively was used. Scanning rate was 2 °C·min<sup>-1</sup>. The initial slit was 2 mm, the detector slit was 0.25 mm. TG and DSC measurements were provided by the STA 449 F3 Netzsch (Germany) device under air atmosphere. The heating rate was 5 °C·min<sup>-1</sup>.

The surface area was determined by the BET method for low-temperature adsorption-desorption of nitrogen. The measurements were provided by the Sorbi-MS (Russia) device. Before the test, the samples were dried in a nitrogen stream at a temperature of 200 °C for 60 min.

SEM microphotographs were provided by the Vega 3 Tescan device with the acceleration voltage of 20 kV and SE detector.

The catalytic activity of the samples was studied in the oxidative dehydrogenation of methanol in a flow-type unit PKU-2. The sample of the catalyst (fraction of 0.25 - 0.50 mm) was loaded into a steel reactor. The composition of the reaction gas environment includes 6.5% methanol and 93.5% air. The volumetric gas velocity was 12500 h<sup>-1</sup>. The temperature in the reactor ranged from 100 to 400 °C. The measurements of gas composition were provided by the Crystallux-4000M device.

### 2.3. Calculating procedures

The interplanar distances (*d*) and the dimensions of the coherent scattering region (CSR) were calculated from XRD data. The identification of crystalline phases on the diffraction pattern was carried out by comparing the calculated interplanar distances with those given in the ASTM database. The interplanar distances were calculated according to the Bragg equation:

$$d = \frac{\lambda}{2 \sin \theta} \quad (1)$$

Where  $\lambda$  is the wavelength,  $\Theta = X_c/2$  is the diffraction angle, which was calculated as the gravity center position of reflex [15]:

$$X_c = \frac{\int_{-\infty}^{+\infty} I(\vartheta) d\vartheta}{I_{max}} \quad \text{or} \quad X_c = \frac{\sum_{i=1}^{N-1} (I_i + I_{i+1}) \Delta\vartheta}{2I_{max}} \quad (2)$$

Where *I* is the intensity at the diffraction angle  $\vartheta$  and *I*<sub>max</sub> is the maximum intensity.

Calculation of the dimension of coherent scattering region (*D*<sub>CSR</sub>) was carried out using the modified Scherrer's equation [16], which has been formed after linearization:

$$\beta_{ph} \cos \theta = \frac{\lambda}{D_{SCR}} + 4\varepsilon \sin \theta \quad (3)$$

Where *D*<sub>SCR</sub> is the dimension of the coherent scattering region,  $\varepsilon$  is the value of the relative mean square micro deformation (MD),  $\beta_{ph}$  is the integral physical broadening of the X-ray sample profile, which was calculated using the Gaussian's function:

$$\beta_s^2 = \beta_{ph}^2 + \beta_{inst}^2 \quad (4)$$

Where  $\beta_s^2$  is the integral broadening of the X-ray profile of the sample,  $\beta_{inst}^2$  is the instrumental broadening. Broadening of the X-ray profile of the etalon was used as instrumental broadening.

Integral broadening of X-ray profile was calculated by the equation:

$$\beta = \frac{\int_{-\infty}^{+\infty} I(\vartheta) d\vartheta}{\int_{-\infty}^{+\infty} I(\vartheta) d\vartheta} \text{ or } \beta = \frac{\sum_{i=1}^{N-1} I_i \vartheta_i}{\sum_{i=1}^N I_i} \quad (5)$$

The interplanar distances and corresponding Miller's indices were used to calculate the unit cell parameters. For tetragonal syngony, the equation has the following form:

$$\frac{1}{d^2} = \frac{H^2 + K^2}{a^2} + \frac{L^2}{c^2} \quad (6)$$

Where  $d$  is the interplanar distance;  $a$ ,  $c$  are the unit cell parameters;  $H$ ,  $K$ ,  $L$  are the Miller's indices.

The integral selectivity of the process ( $S$ ) for the product was estimated as the ratio of the amount of methanol converted to the final product ( $N_{Me}$ ) to the total amount of methanol converted ( $\Delta N_{Me}$ ):

$$S = \frac{N_{Me-r}}{\Delta N_{Me}} \quad (7)$$

### 3. Results and Discussion

#### 3.1. Catalyst structure, morphology and characteristics

As a result of the mechanical activation of SnO<sub>2</sub> and h-MoO<sub>3</sub> oxides, two types of processes occur and lead to distortion of the tin oxide crystal lattice. The first

process is accompanied by introducing of Mo atoms into interstitial spaces (voids) of the SnO<sub>2</sub>. The second process is the formation of defects in the structure of a solid body due to thermal activation. It was established that increasing the time of mechanical activation can remove the reflexes of the h-MoO<sub>3</sub> phase and shift the SnO<sub>2</sub> phase reflections gradually toward to smaller angles. It indicates that the crystal structure of tin oxide is deformed, and the lattice parameters gradually decrease. The phase composition depends on the components and the time of mechanical activation (Fig. 1). Thus, samples subjected to MA with the SnO<sub>2</sub>:h-MoO<sub>3</sub> molar ratios of 2.3:1 and 5.7:1 are single-phase, there are only characteristic reflections of the SnO<sub>2</sub> phase on the XRD patterns. The samples with higher content of MoO<sub>3</sub> leads to the presence of free h-MoO<sub>3</sub> in the mixture subjected to mechanical activation.

Morphology of prepared catalysts has been determined by SEM instruments. Fig. 2 can reveal the formation of spherical like structures in the SnO<sub>2</sub>:h-MoO<sub>3</sub> catalyst, with the particle size of 0.1-0.2 μm, which form denser flaky aggregates with size of 0.5-2 μm. The ratio change of the initial components does not lead to significant changes in the overall morphology of the samples.

Tin oxide has a tetragonal unit cell with the parameters  $a = b = 4,745 \text{ \AA}$ ,  $c = 3,192 \text{ \AA}$ . It should be noted that the crystal lattice of tin oxide undergoes deformation in the process of mechanical activation, caused both by intense mechanical influences and by the introduction of molybdenum atoms into the structure of SnO<sub>2</sub>. Therefore, the change in the specific volume of tin oxide unit cell has a wavy characteristic (Fig. 3).

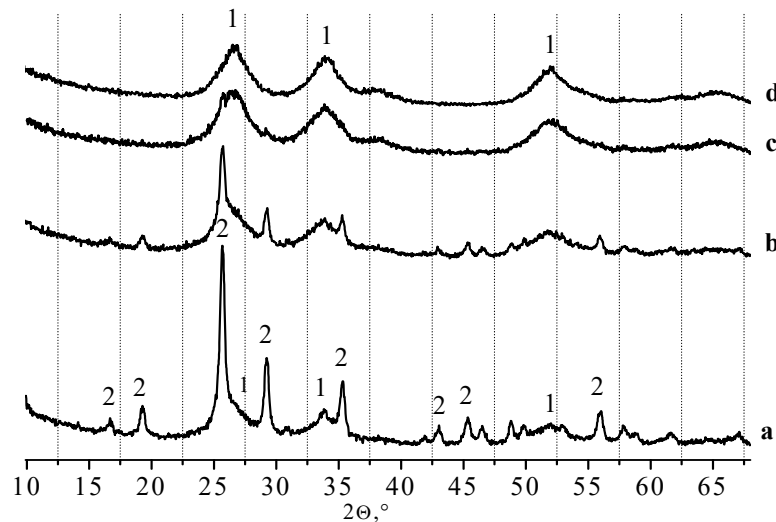


**Fig. 1.** XRD patterns of the MA products of SnO<sub>2</sub> (1) and h-MoO<sub>3</sub> (2) mixture at the activation time of 60 min. SnO<sub>2</sub>:h-MoO<sub>3</sub> ratios: a – 1:2.3; b – 1:1; c – 2.3:1; d – 5.7:1.  $2\theta$  – diffraction angle, degrees.

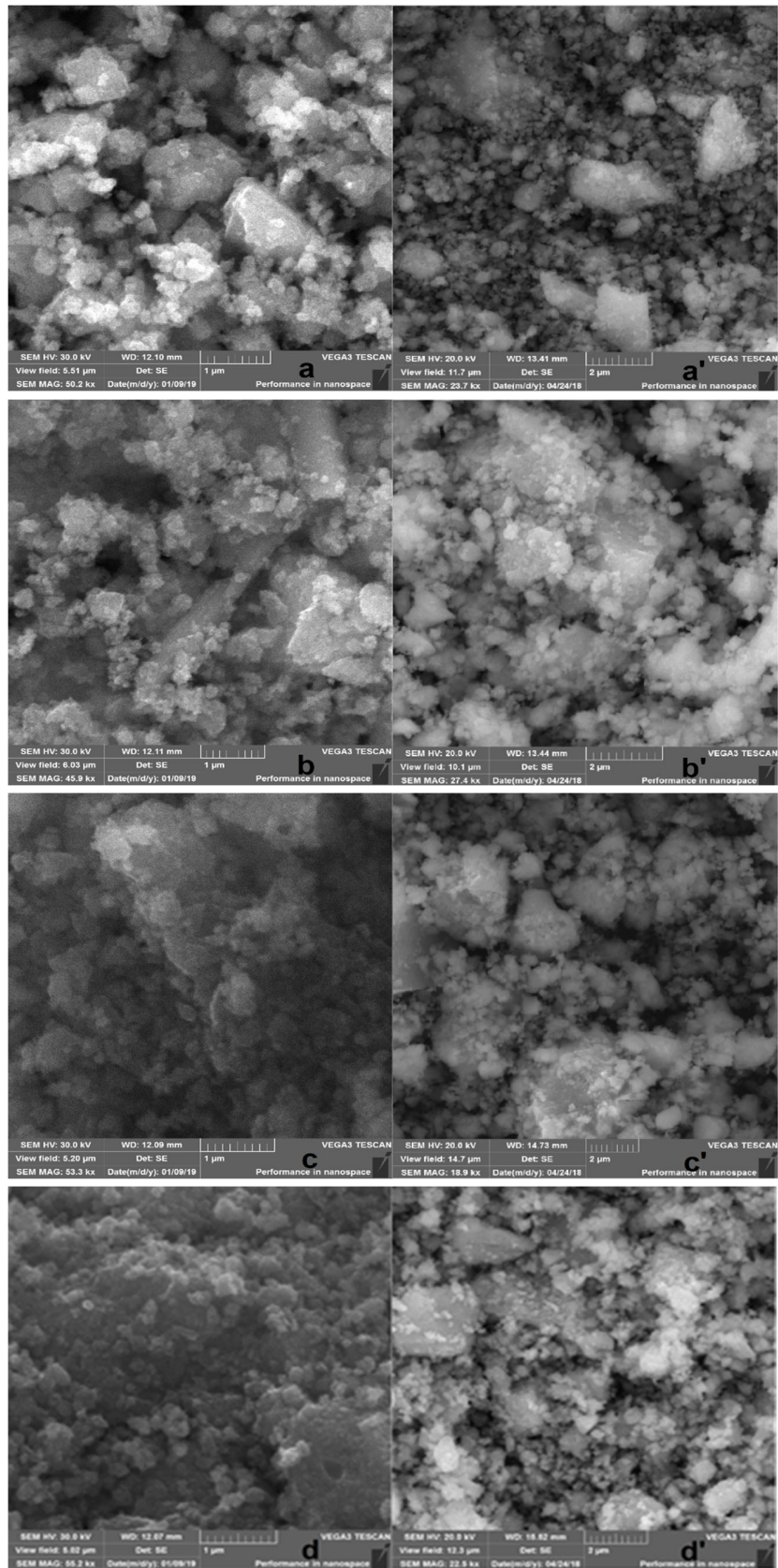


**Fig. 2.** SEM images of products of mechanical activation of SnO<sub>2</sub> and h-MoO<sub>3</sub> mixture during 60 min. SnO<sub>2</sub>:h-MoO<sub>3</sub> ratios: a, a' - 1:2.3; b, b' - 1:1; c, c' - 2.3:1; d, d' - 5.7:1.

Thus, the process of joint mechanical activation can be divided into three stages. In the first stage, the grinding and activation of tin oxide occurs, accompanied by the crystal lattice parameters and volume decreasing. At the second stage, an increase of the unit cell volume occurred due to the introduction of molybdenum atoms and their distribution in the SnO<sub>2</sub> crystal lattice, i.e. formation of tin-molybdenum solid solution. The third stage is associated with the ongoing processes of plastic deformation of the crystalline without significant changes in the unit cell volume.

The calculation of the CSR sizes shows similar dependences. Thus, the initial tin oxide has the following characteristics: the surface area is 170 m<sup>2</sup>/g, the average CSR size is 65 Å. The joint mechanical activation of the SnO<sub>2</sub>:h-MoO<sub>3</sub> system during 15 min leads to reducing of the CSR average size to 30 Å. Then its value increases up to 40 Å when oxides get activated during 35 min. After that, the influence of the activation time decreases.

Analysis of the specific surface area of SnO<sub>2</sub>:h-MoO<sub>3</sub> mixture after mechanical activation decreases when the MoO<sub>3</sub> content in the mixture increases (Table 1). Thus, the introduction of Mo atoms into the SnO<sub>2</sub> structure leads to the formation of a solid solution and is accompanied by a decrease in the number of micropores. Based on the XRPA data, it is possible to make some assumptions about the physical interaction of SnO<sub>2</sub> and h-MoO<sub>3</sub> in the process of mechanical activation. During the thermal activation, the particles of molybdenum oxide (Mohs hardness of 4.5, S<sub>sp</sub> = 3.0 m<sup>2</sup>/g [17]) are powdered on the surface of SnO<sub>2</sub> (Mohs hardness of 7 [17]) with the higher specific surface (S<sub>sp</sub> = 180.2 ± 3.7 m<sup>2</sup>/g).

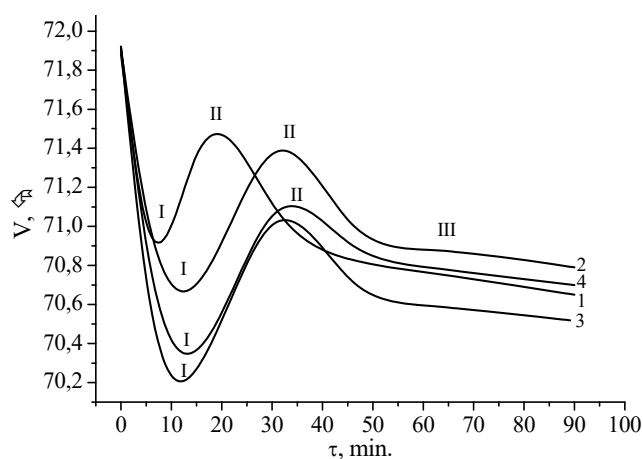


**Fig. 3.** Change in the unit cell volume of SnO<sub>2</sub> in the process of joint mechanical activation with h-MoO<sub>3</sub>. SnO<sub>2</sub>:h-MoO<sub>3</sub> ratios: 1 – 5.7:1; 2 – 2.3:1; 3 – 1:1; 4 – 1:2.3.  $\tau$  – MA time, min; V – unit cell volume, Å.

**Table 1.** Effect of the SnO<sub>2</sub>:h-MoO<sub>3</sub> ratio on the surface area.

SnO <sub>2</sub> :h-MoO <sub>3</sub> ratio	Surface area (m <sup>2</sup> /g)
SnO <sub>2</sub> :MoO <sub>3</sub> = 1:2,3	12.27
SnO <sub>2</sub> :MoO <sub>3</sub> = 1:1	13.93
SnO <sub>2</sub> : MoO <sub>3</sub> = 2,3:1	48.12
SnO <sub>2</sub> : MoO <sub>3</sub> = 5,7:1	64.04

SnO<sub>2</sub> powder is characterized by a mesoporous structure with a narrow pore distribution from 2 to 30 nm. Since molybdenum oxide covers the surface of tin oxide, pore blocking occurs and, as a result, the specific surface area decreases.

### 3.2. Catalyst thermal behavior

Heat treatment of a sample subjected to mechanical activation within 60 minutes is accompanied by weight loss of 6-8% up to a temperature of 750 °C (Fig. 4). The decrease of the samples mass is due to the removal of both water and carbon dioxide physically adsorbed from the air, and the removal of crystallization water from SnO<sub>2</sub>·nH<sub>2</sub>O. In addition, h-MoO<sub>3</sub> also contains an insignificant amount of moisture [18], which removal is observed up to the recrystallization temperature of h-MoO<sub>3</sub> into  $\alpha$ -MoO<sub>3</sub>. The process of heat treatment of the samples is also accompanied by several thermal effects, the number of which depends on the SnO<sub>2</sub>:h-MoO<sub>3</sub> ratio. So, the first and the second thermal effects lying in the temperature range of 20-245 °C are associated with the removal of water and carbon dioxide, which were physically adsorbed from the environment during the mechanical activation. The third thermal effect is exothermic, which is well manifested only on samples containing 50% or more of h-MoO<sub>3</sub> phase, because of polymorphic transformation of h-MoO<sub>3</sub> into  $\alpha$ -MoO<sub>3</sub>.

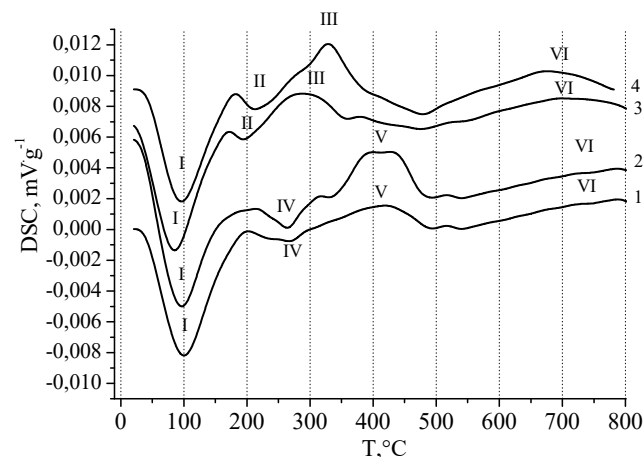


**Fig. 4.** Synchronous thermal analysis of the products of mechanical activation of the SnO<sub>2</sub>:h-MoO<sub>3</sub> mixture. SnO<sub>2</sub>:h-MoO<sub>3</sub> ratios: 1 – 5.7:1; 2 – 2.3:1; 3 – 1:1; 4 – 1:2.3.

The fourth thermal effect is endothermic effect which was caused by the removal of crystallization water from  $\text{SnO}_2 \cdot n\text{H}_2\text{O}$ . The fifth thermal effect is exothermic; it is strongly stretched and observed only in cases of  $\text{SnO}_2$  excess, due to the crystallization of the tin oxide phase. The sixth thermal effect is exothermic, it is also strongly stretched and caused by the formation and crystallization of tin molybdate.

XRD phase analysis of the products of mechanical activation of  $\text{SnO}_2$ :h- $\text{MoO}_3$  mixture calcined at 750 °C indicates the formation of a well-crystallized  $\text{Sn}(\text{MoO}_4)_2$  tin molybdate (Fig. 5), amount of which depends on the  $\text{SnO}_2$ :h- $\text{MoO}_3$  ratio. The characteristic reflections of the  $\alpha$ - $\text{MoO}_3$  phase are present on the XRD patterns. Reduction of the h- $\text{MoO}_3$  fraction in the mixture to be activated to 15 wt.% does not cause a significant change in the XRD patterns before and after calcination, and only the strongly broadened reflexes of the  $\text{SnO}_2$  phase are observed.

However, the formation of the  $\text{Sn}(\text{MoO}_4)_2$  phase is supported by synchronous thermal analysis data. Obviously, during the thermal treatment of  $\text{SnO}_2$ :h- $\text{MoO}_3$  mixture, the molar ratio of 5.7:1, there are two opposite processes: the formation of tin molybdate and the formation of a solid solution in the  $\text{SnO}_2$  lattice.

Microphotographs of  $\text{SnO}_2$  and h- $\text{MoO}_3$  mixture mechanically activated and treated at 750 °C are presented in Fig. 6. Calcination of the samples does not lead to a significant change in the morphology of the particles. However, preliminary mechanical activation of samples thermally treated can enhance the dimensions of both the particles themselves and the aggregates they formed.

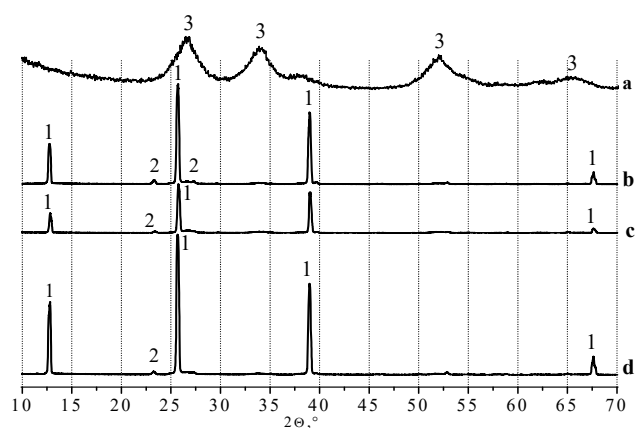
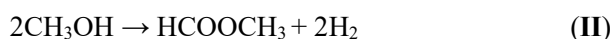
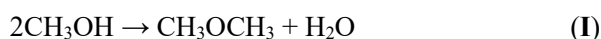


**Fig. 5.** XRD patterns of the products of mechanical activation of  $\text{SnO}_2$ :h- $\text{MoO}_3$  mixture calcined at 750 °C. 1- $\text{Sn}(\text{MoO}_4)_2$ , 2- $\alpha$ - $\text{MoO}_3$ , 3- $\text{SnO}_2$ .  $\text{SnO}_2$ :h- $\text{MoO}_3$  ratios: a – 5.7:1; b – 1:1; c – 2.3:1; d – 1:2.3.  $2\theta$  – diffraction angle, degrees.

### 3.3. Catalytic properties

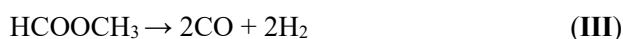
The catalytic properties of the obtained samples of tin-molybdenum catalysts were investigated in the reaction of oxidative dehydrogenation of methanol (Fig.7 a-d).

When methanol is converted into an oxygen-containing medium, samples of a tin-molybdenum catalyst undergo reactions to form dimethyl ether (DME) and methyl formate (MF) in accordance with the following reactions:



The formation of methyl formate on all samples of the catalyst begins at a temperature of about 120 °C. It should be noted that the selectivity of the methyl formate formation reaches 91 % at 215 °C on the sample containing 30 wt. % of  $\text{MoO}_3$ . The increase in the content of molybdenum oxide in the samples to 70 wt. % leads to a decrease in selectivity, however, the temperature range for the formation of methyl formate expands significantly. Thus, the selectivity of the process of formation of methyl formate and its temperature range substantially depend on the content of molybdenum oxide in the catalyst.

The selectivity of the dimethyl ether formation has an extreme nature. Since the formation of dimethyl ether is exothermic, its equilibrium concentration decreases with the increase of temperature (Fig. 7 a-d). This explains the decrease in the selectivity for DME with increasing temperatures (Fig. 7). These facts are due to the decomposition of MF to carbon monoxide and hydrogen (III) [19-21].



Such gases as  $\text{CO}$ ,  $\text{CO}_2$  and  $\text{H}_2$  can be formed during the implementation of various routes:

- Direct decomposition of methanol to carbon monoxide and hydrogen;



- Conversion of carbon monoxide. The source of water for this route is the reaction (I);



- Decomposition of MF according to the reaction (III).

Thus, different  $\text{SnO}_2$ :h- $\text{MoO}_3$  ratios in a catalyst lead to a partial suppression of the DME formation route and its shift to higher temperatures.

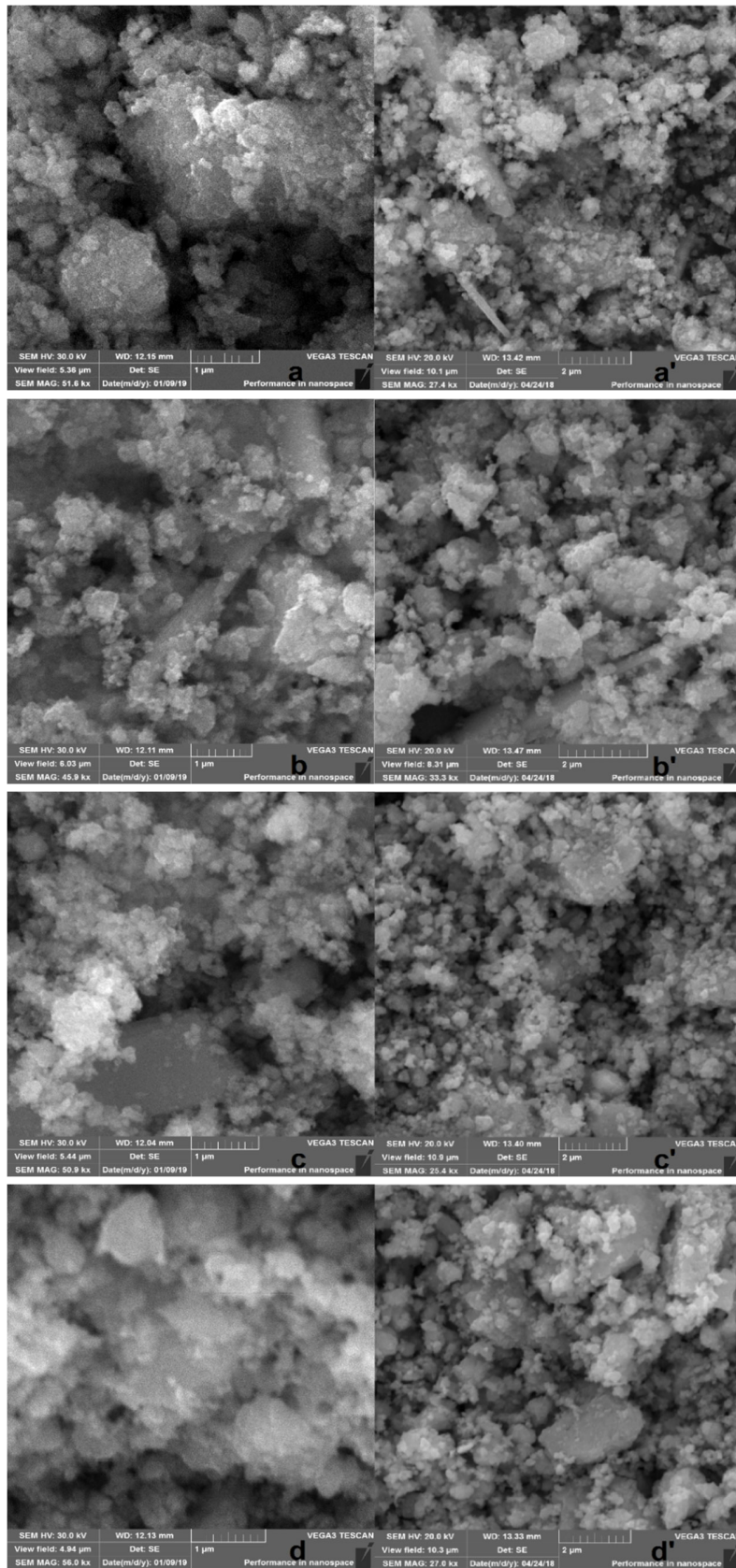


**Fig. 6.** SEM images of products of the heat treatment of SnO<sub>2</sub> and h-MoO<sub>3</sub> mixture at 750 °C. Time of mechanical activation is 60 min. SnO<sub>2</sub>:h-MoO<sub>3</sub> ratios: a – 1:2.3; b – 1:1; c – 2.3:1; d – 5.7:1.

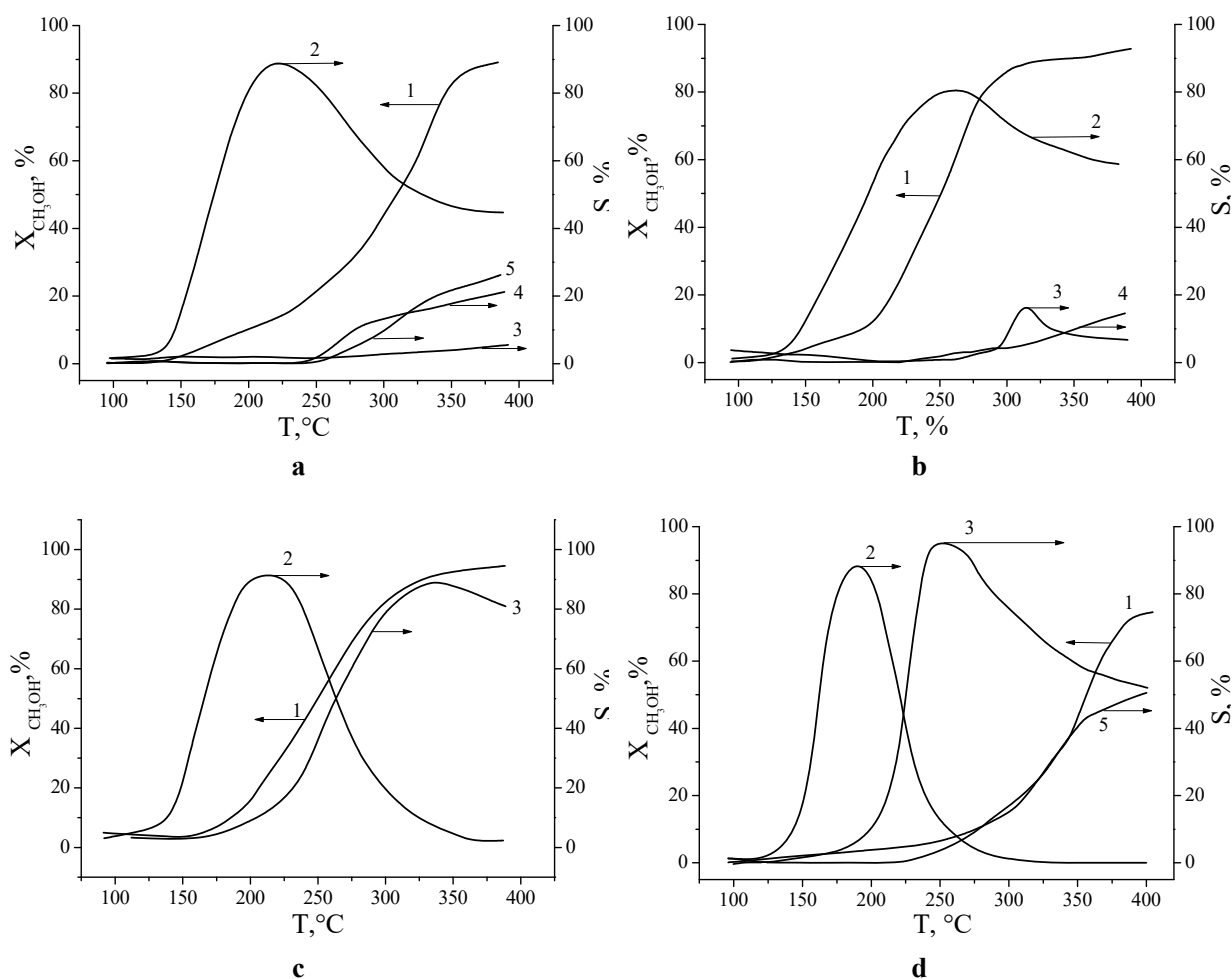


**Fig. 7.** Catalytic properties of the samples obtained.  $\text{SnO}_2$ :h- $\text{MoO}_3$  ratio: a - 1:2,3; b -1:1; c - 2,3:1; d - 5,7:1. 1 – Methanol, 2 – MF, 3 – DME 4 – CO, 5 –  $\text{CO}_2$ .

#### 4. Conclusions

It was concluded that during the mechanical activation process an intensive grinding, breaking and deformation of M-O bonds occurs, and also a solid solution of the introduction of molybdenum atoms in the structure of  $\text{SnO}_2$  is formed. It is shown that the formation of a solid solution during mechanical activation occurs in three stages and is accompanied by deformation of the  $\text{SnO}_2$  crystal lattice. Thermal treatment of mechanically activated the mixture in the temperature range of 600-750 °C, this leads to the formation of crystalline  $\text{Sn}(\text{MoO}_4)_2$ .

Varying the  $\text{SnO}_2$ :h- $\text{MoO}_3$  ratio allows adjusting the selectivity of the methanol conversion process to methyl formate and dimethyl ether. This effect is due to the decrease in acidity of the catalyst surface and the formation of the base centers, which were together provided for the dehydrogenation of methanol to form aldehyde groups [12, 22, 23].

#### Acknowledgements

The investigation was funded by the Ministry of Education and Science of the Russian Federation according to the research project No 3.1371.2017/4.6 and partially supported with the scholarship of the President of the Russian Federation for young scientists and graduate students who carry out advanced research and development in priority areas of modernization of the Russian economy (2016-2018 years) according to No SP-3477.2016.1. The resources of the Center for the collection of scientific equipment of the Ivanovo State University of Chemistry and Technology (ISUCT) were used for the research.

#### References

- [1] R.N. Rumyantsev, A.A. Il'in, A.P. Il'in, I.V. Pazukhin, *Theor. Exp. Chem.* 47 (2011) 41-44.
- [2] T.G. Alkhozov, K.Y.U. Adzhamov, F.M. Poladov, *React. Kinet. Catal. Lett.* 7 (1977) 65-68.
- [3] F.J. Berry, C. Hallett, *Inorg. Chim. Acta.* 98 (1985) 69-72.



- [4] S.T. Yoshihiko, M. Atsumu Ozaki, *J. Catal.* 17 (1970) 132-142.
- [5] L.V. Bogutskaya, S.V. Khalameida, A.V. Zazhigalov, A.I. Kharlamov, L.V. Lyashenko, O.G. Byl', *Theor. Exp. Chem.* 35 (1999) 242-246.
- [6] M. Ai, *J. Catal.* 77 (1982) 279-288.
- [7] M. Bowker, A.F. Carley, M. House, *Catal. Lett.* 120 (2008) 34-39.
- [8] M.P. House, M.D. Shannon, M. Bowker, *Catal. Lett.* 122 (2008) 210-213.
- [9] E. Söderhjelm, M.P. House, N. Cruise, J. Holmberg, M. Bowker, J.-O. Bovin, A. Andersson, *Top. Catal.* 50 (2008) 145-155.
- [10] A.A. Il'in, K.K. Dao, R.N. Rumyantsev, A.P. Il'in, K.A. Petukhova, V.A. Goryanskaya, *Russ. J. Appl. Chem.* 90 (2017) 1433-1438.
- [11] T.G. Alkhazov, K.Y.U Adzhamov, F.M. Poladov, *React. Kinet. Catal. Lett.* 7 (1977) 65-68.
- [12] A.A. Davydov, *React. Kinet. Catal. Lett.* 19 (1982) 377-382.
- [13] H. Kösea, A.O. Aydına, H. Akbulutb, *Acta Phys. Pol. A.* 125 (2014) 345-347.
- [14] E.G. Avvakumov, M. Senna, N.V. Kosova, *Soft mechanochemical synthesis*, Springer, Boston, 2001.
- [15] G. Ludwig, *Untersuchungsmethoden zur Charakterisierung Mechanisch Aktivierten Festkörpern*, ed by Z. Juhasz, Közdotk Pubk., Budapest, (1978), p. 113-198.
- [16] T. Ekström, C. Chatfield, W. Wruss, J. Maly-Schreiber, *Mater. Sci.* 20 (1985) 1266-1274.
- [17] W. Shumann, *Minerals of the world*, Sterling Publishing Company, Inc. (2008). p. 549.
- [18] I.V. Babichev, A.A. Il'in, R.N. Rumyantsev, N.E. Nikonorova, A.P. Il'in, *Russ. J. Appl. Chem.* 87 (2014) 298-302.
- [19] M. Ai, *Appl. Catal.* 11 (1984) 259-270.
- [20] T.P. Minyukova, I.I. Simentsova, A.V. Khasin, N.V. Shtertser, N.A. Baronskaya, A.A. Khassin, T.M. Yurieva, *Appl. Catal. A* 237 (2002) P.171-180.
- [21] L. Shlegel, D. Gushtik, A.I. Rozovskii, *Kinet. Catal.* 31 (1990) 1000-1003.
- [22] A. Lycourghiotis, D. Vattis, P. Aroni, N. Katsanos, *Z. Phys. Chem. Neue Fol.* 121 (1980) 257-265.
- [23] E.A. Makeeva, M.N. Rumyantseva, A.M. Gas'kov, *Inorg. Mater.* 41 (2005) 370-377.